

Towards a unified understanding of jet-quenching and elliptic flow within perturbative QCD parton transport

Oliver Fochler,¹ Zhe Xu,¹ and Carsten Greiner¹

¹*Institut für Theoretische Physik, Goethe-Universität Frankfurt am Main
Max-von-Laue-Straße 1, D-60438 Frankfurt am Main, Germany*

The gluonic contribution to the nuclear modification factor, R_{AA} , is investigated for central Au+Au collisions at $\sqrt{s} = 200$ AGeV employing a perturbative QCD-based parton cascade including radiative processes and found to be in good agreement with results from the GLV formalism. We demonstrate that the present microscopic transport description is able, for the first time, to explain both jet-quenching and a strong build-up of elliptic flow in terms of the same standard perturbative QCD interactions.

PACS numbers: 12.38.Mh, 24.10.Lx, 24.85.+p, 25.75.-q, 25.75.Bh

The phenomenon of jet-quenching [1] has been one of the two striking discoveries at the Relativistic Heavy Ion Collider (RHIC) [2, 3]. It is widely believed to provide tomography of the quark-gluon plasma (QGP) created in ultra-relativistic heavy ion collisions. Furthermore, the strong elliptic flow, quantified by the Fourier parameter v_2 , explores the early bulk properties of the medium. Since ideal hydrodynamics can fairly reproduce the observed v_2 -dependence on centrality [4], viscosity in the QGP is believed to be small [5, 6]. Hence, the QGP behaves like a perfect fluid, which has been the second major discovery at RHIC. So far, it has not been possible to relate both phenomena by a common understanding of the underlying microscopic processes.

Attempts to understand the collective behavior by means of standard binary, elastic perturbative QCD (pQCD) collisions within a parton cascade has failed unless (unphysically) large cross sections are employed [7, 8]. With such cross sections, as we will also demonstrate in the following, the attenuation of the jets would be far too strong, basically extinguishing all high-momentum partons. Also, there exist several related theoretical schemes of the energy loss on the partonic level including radiative pQCD interactions aiming at describing the observed amount of jet-quenching [9, 10, 11, 12, 13, 14]. In particular the energy loss is found to be dominantly radiative. It is thus believed that different microscopic physics become manifest in perturbative interactions of jet particles with bulk particles on the one hand, and in seemingly much stronger interactions of medium constituents among each other on the other hand, giving rise to the liquid-like bulk properties.

It has been recently demonstrated within BAMPS [15, 16] (A Boltzmann approach to multi parton scatterings), a more sophisticated kinetic pQCD based parton cascade *including radiative contributions*, that inelastic Bremsstrahlung processes can drive the system to equilibration within a short time less than 1 fm/c. Moreover, pQCD Bremsstrahlung processes generate a sizeable degree of collective flow [17] and a small ratio of shear vis-

cosity to entropy density η/s . Using parton-hadron duality the simulated elliptic flow coefficient v_2 has been demonstrated to be in fair agreement with data employing a coupling constant $\alpha_s = 0.3 \div 0.6$. Some minor details on freeze-out, hadronization and possible hadronic phase contributions have still to be addressed. For the created gluon plasma η/s is in the range $0.08 \div 0.15$, supporting the idea that the medium behaves like a nearly ideal fluid [17, 18].

The present study is motivated by the challenging question whether the employed treatment of pQCD interactions, including radiative processes, can simultaneously account for the quenching of high-momentum partons.

Microscopic transport calculations provide a realistic way of understanding heavy ion collisions including the full dynamical evolution of the system and allowing for non-thermal initial conditions. We employ BAMPS to investigate the evolution of gluon matter produced in heavy ion collisions at RHIC. Treating gluons as semi-classical and massless Boltzmann particles, elastic $gg \rightarrow gg$ interactions are included via the leading order pQCD differential cross section $\frac{d\sigma_{gg \rightarrow gg}}{dq_\perp^2} = \frac{9\pi\alpha_s^2}{(\mathbf{q}_\perp^2 + m_D^2)^2}$. The effective Bremsstrahlung matrix element

$$|\mathcal{M}_{gg \rightarrow ggg}|^2 = \frac{72\pi^2\alpha_s^2 s^2}{(\mathbf{q}_\perp^2 + m_D^2)^2} \frac{48\pi\alpha_s \mathbf{q}_\perp^2}{\mathbf{k}_\perp^2 [(\mathbf{k}_\perp - \mathbf{q}_\perp)^2 + m_D^2]} \times \Theta\left(\frac{\Lambda_g}{\gamma} - \tau\right) \quad (1)$$

is used for inelastic gluon multiplication and annihilation processes. \mathbf{q}_\perp and \mathbf{k}_\perp denote the perpendicular components of the momentum transfer and of the radiated gluon momentum in the center of mass (CM) frame of the colliding particles, respectively. Gluon interactions are screened by a Debye mass $m_D^2 = d_G \pi \alpha_s \int \frac{d^3p}{(2\pi)^3} \frac{1}{p} N_c f$, where $d_G = 16$ is the gluon degeneracy factor for $N_c = 3$, and which is dynamically computed from the local distribution function $f(p, x, t)$.

In the treatment of Bremsstrahlung processes the coherent Landau, Pomeranchuk and Migdal (LPM) effect

[19], leads to a suppression of the emission rate for very high energy particles. In principle, such interference effects cannot be included in the microscopic transport calculations. Therefore, the Theta function in (1) is introduced to ensure that only independent processes are considered, i.e. that only processes within the so called Bethe-Heitler regime are taken into consideration. Physically this implies that the formation time τ of the emitted gluon must not exceed the mean free path of the parent particle. The mean free path Λ_g is given in the local comoving frame of a computational spatial cell, which is not identical with the frame where the gluon is emitted purely transversal and thus $\tau = 1/k_\perp$. A Lorentz factor $\gamma = \frac{\cosh y}{\sqrt{1-\beta^2}} (1 + \beta \tanh y \cos \theta)$ has to be employed. β denotes the boost velocity from the comoving frame to the CM frame of the colliding particles, y is the rapidity of the emitted gluon measured from the CM frame and θ is the angle between $\vec{\beta}$ and the axis of the colliding particles in the CM frame. For thermal particle energies the boost β becomes small and the Theta function reduces to $\Theta(k_\perp \Lambda_g - \cosh y)$.

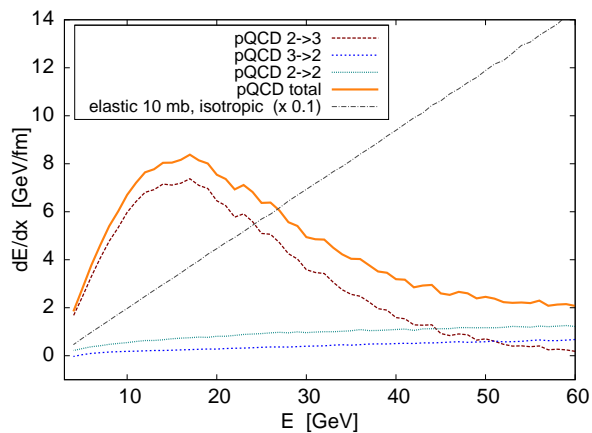


FIG. 1: (Color online) Differential energy loss of a gluon jet in a static and thermal medium of gluons with $T = 400$ MeV. The contributions of the different pQCD processes to the total dE/dx are shown. Additionally dE/dx scaled down by a factor of 10 is shown for a gluon jet interacting only via isotropic binary scatterings with a fixed cross section $\sigma = 10$ mb.

The cut-off in (1) affects the overall value of the interaction probability for $gg \leftrightarrow ggg$ as well as the momentum shape of the spectrum of the radiated gluons. The larger γ , the smaller the emission probability. Fig. 1 shows the differential energy loss dE/dx of a high energy gluon jet in a static and thermal medium of gluons with temperature $T = 400$ MeV as a function of the jet energy E . Throughout this work we employ a coupling constant $\alpha_s = 0.3$. The elastic energy loss from $gg \rightarrow gg$ interactions is found to be approximately constant at a level of $dE/dx = 1.5 \div 1.2$ GeV/fm and the contribution from $ggg \rightarrow gg$ processes is even smaller with $dE/dx = 1.0 \div 1.5$ GeV/fm. Over a wide energy range ra-

diative $gg \rightarrow ggg$ processes strongly dominate the energy loss resulting in a maximum total $dE/dx \approx 8.5$ GeV/fm at $E \approx 15$ GeV. The drop of the radiative contribution to higher jet energies originates from the effective LPM cut-off introduced in (1). With rising jet energy the boost γ to the CM frame rises, leading to a stronger suppression of these emissions. For very high jet energies $E \gtrsim 45$ GeV the radiative contribution in our scheme becomes even less important than the elastic energy loss. At such energies, the effective implementation of the LPM effect is probably rather crude, leading potentially to an underestimation of the actual radiative energy loss.

For arguments to come, Fig. 1 also shows dE/dx (scaled down by a factor of 10) for a gluon jet interacting purely elastic with the medium at a fixed exemplary cross section of $\sigma = 10$ mb and an isotropic angular distribution. The differential energy loss in this case rises linearly with the jet energy E and is much larger than dE/dx from pQCD interactions, e.g. $dE/dx|_{\sigma=10 \text{ mb}} \approx 37$ GeV/fm at $E = 15$ GeV.

The initial gluon distribution for Au+Au collisions at 200 AGeV is chosen to be an ensemble of mini-jets with a lower momentum cut-off $p_0 = 1.4$ GeV, produced in nucleon-nucleon collisions following a Glauber-model with a Wood-Saxon density profile and Glück-Reya-Vogt parton distribution functions [20] with a K -factor of 2. Free streaming is applied to regions where the energy density has dropped below a critical energy density of $\varepsilon_c = 1$ GeV/fm³. The evolution of the fireball is simulated until the energy density has dropped below ε_c . With this setup it has been demonstrated [15] that the experimental findings for the rapidity distribution of transverse energy and the flow parameter for various centralities are nicely reproduced.

Due to the steeply falling momentum spectrum of the initial jets one would need to simulate an infeasible high number of events in order to obtain sufficient statistics at high- p_T . One therefore has to develop a suitable weighting and reconstruction scheme. The underlying idea is to simulate a huge number of *initial spectra*, which is rather straightforward from the computational point of view, and to select such events for further simulations that contain high- p_T partons. The results then need to be appropriately weighted. For this we characterize each initial state according to $X = \max(p_{T,i})$, the maximum p_T in a given rapidity range. From each bin j in X a number of N_j events is simulated, the results are averaged within these bins and finally combined with appropriate weights P_j . This procedure has been thoroughly tested [23] and, so far, allows for the investigation of observables up to $p_T \approx 30$ GeV. In the following we use a bin-size of 1 GeV and select up to $N_j = 160$ events per bin for full simulation.

Jet-quenching is generally specified in terms of the nu-

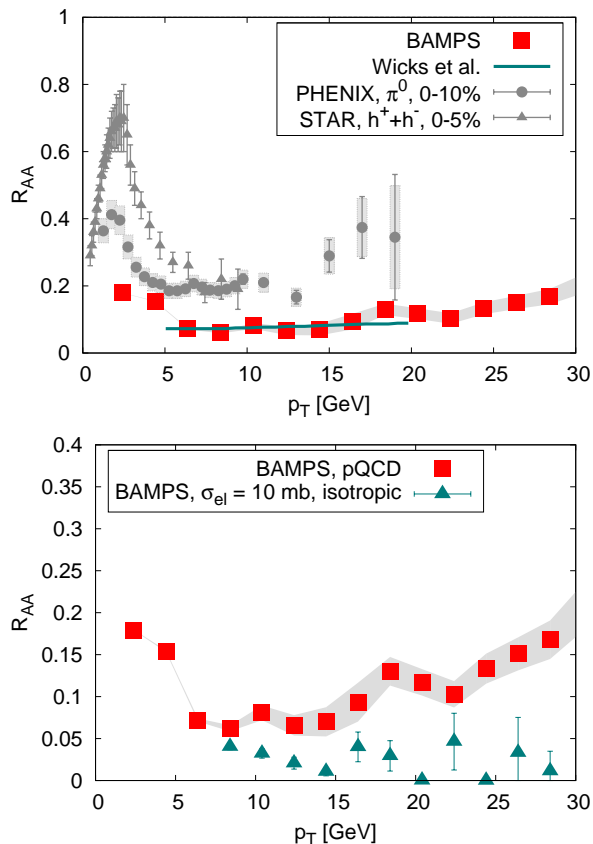


FIG. 2: (Color online) Upper: Gluonic R_{AA} at midrapidity ($y \in [-0.5, 0.5]$) as extracted from simulations for central Au+Au collisions at 200 AGeV. The shaded area indicates the statistical error. For direct comparison the result from Wicks et al. [14] for the gluonic contribution to R_{AA} and experimental results from PHENIX [21] for π^0 and STAR [22] for charged hadrons are shown. Lower: Gluonic R_{AA} (triangles) for a scenario where all particles with $p_T > 8$ GeV can only interact elastically with fixed $\sigma = 10$ mb.

clear modification factor

$$R_{AA} = \frac{d^2 N_{AA}/dp_T dy}{T_{AA} d^2 \sigma_{NN}/dp_T dy}, \quad (2)$$

which is the ratio of the particle yield in a A+A collision at given p_T and y to the yield in a p+p collision scaled by the appropriate number of binary collisions. We directly compute R_{AA} by taking the ratio of the final p_T spectra to the initial mini-jet spectra. In this letter we concentrate on central ($b = 0$ fm) collisions, R_{AA} for non-central collisions can be straightforwardly studied and will be presented in an upcoming work [23]. Fig. 2 shows the result for the gluonic contribution to R_{AA} , exhibiting a clear suppression of high- p_T gluon jets at a roughly constant level of $R_{AA}^{\text{gluons}} \approx 0.1$, potentially slightly rising towards high p_T . This constitutes the major result of the present study.

The suppression is approximately a factor two stronger than the experimental pion data. This, however, was to be expected since at present the simulation does not in-

clude quarks, which are expected to lose less energy by a factor of 4/9. Indeed, comparing with state of the art results from Wicks et al. [14] for the gluonic contribution to R_{AA} (seen as the line in Fig. 2), which in their approach together with the quark contribution reproduces the experimental data, one finds a perfect agreement. In their calculation a gluon density per unit rapidity of $dN_g/dy = 1100$ is assumed and the strong expansion of the fireball has to be effectively modeled. In the present microscopic treatment the full dynamics are selfconsistently included, where the initial gluon density is given by $dN_g/dy \approx 700$, which then evolves to $dN_g/dy \approx 800$. The inclusion of light quarks will provide further means of verification and will be addressed in a future work.

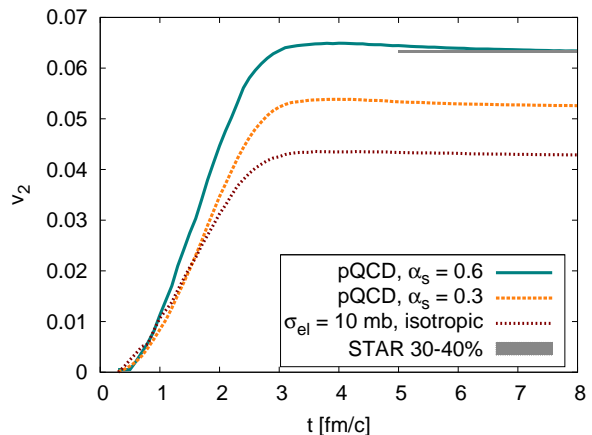


FIG. 3: (Color online) Generation of elliptic flow at midrapidity for a noncentral collision with an impact parameter of $b = 8.6$ fm [17]. The result employing only binary collisions with constant $\sigma = 10$ mb are also shown for comparison. The grey-shaded band represents the experimental value [24].

To demonstrate the importance of inelastic processes for explaining both elliptic flow and jet-quenching on the same footing, in Fig. 3 we compare the elliptic flow for a scenario of only binary and isotropic collisions with $\sigma = 10$ mb to the full results from [17]. Though the cross section is large, it still does not fully succeed in explaining the strong elliptic flow. A still larger one has to be (phenomenologically) employed in order to generate enough flow [7, 8]. On the other hand, we also investigate a scenario in which jet-like gluons with $p_T > 8$ GeV can only interact elastically with the same fixed and isotropic cross section of $\sigma = 10$ mb. In this calculation, the medium particles interact with the usual pQCD based matrix elements, including inelastic collisions. As already expected from Fig. 1, the results shown in the lower panel of Fig. 2 explicitly demonstrate that the suppression in this case is far too strong by almost an order of magnitude. So, while approaches using fixed and large cross sections might be able to reproduce thermalization times, angular correlations [25] or elliptic flow [7, 8, 26], they would clearly fail at simultaneously reproducing the correct nuclear modi-

fication factor.

The use of a full microscopic transport treatment also offers the possibility to investigate observables, that are not directly accessible in experiment but are useful for visualizing the details of microscopic processes. Fig. 4 shows the probability distribution of production points in the transverse plane of gluon jets with a final $p_T > 15$ GeV in a central ($b = 0$ fm) Au+Au collision using the full pQCD BAMPS version. Events in this illustration are rotated such that the jets emerge with their final \vec{p}_T parallel to the x -axis and directed in positive x -direction. The spatial extent of the initial production points is roughly controlled by the parameter R_A in the Wood-Saxon distribution $n_A(r) = n_0/(1 + e^{(r-R_A)/d})$, with $R_A = 6.37$ fm in our case. A bias towards production points near the surface is visible as would be naively expected for the strong jet suppression seen in Fig. 2. The jets do propagate on the average an effective length of approximately 2 fm. Still, at such high transverse momenta some fewer jets can indeed probe the interior of the reaction volume, indicating that the picture of pure surface emission is oversimplified.

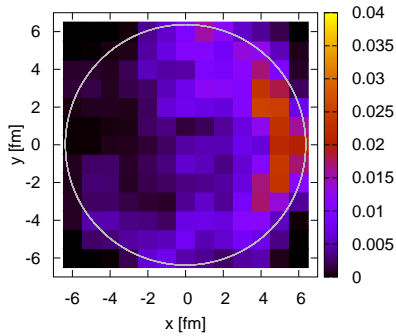


FIG. 4: (Color online) Probability distribution of production points of jets with final $p_T > 15$ GeV. Events are rotated such that jets in the final state travel in the positive x -direction.

We have demonstrated for the first time that a consistent and fully pQCD based microscopic parton transport description is able to quantitatively reproduce both elliptic flow and jet-quenching observed in RHIC experiments within one common setup. The present approach thus constitutes a first realistic 3+1 dim. microscopic transport simulation that can understand both phenomena by the same underlying processes. As established previously, the gluon matter simulated in the parton cascade BAMPS exhibits a sizeable pressure build-up and a small ratio of shear viscosity to entropy, η/s . In this work we found that the suppression of high- p_T gluon jets is roughly constant at $R_{AA}^{\text{gluons}} \approx 0.1$ over a large p_T range, in good accordance with recent analytic results. The consistent inclusion of inelastic $gg \leftrightarrow ggg$ processes is crucial to this finding. Of course, there is room for further improvements: incorporation of light quarks, a more

sophisticated treatment of Bremsstrahlung contributions and the LPM effect.

The authors would like to thank M. Gyulassy for stimulating discussions throughout this work. The simulations were performed at the Center for Scientific Computing of Goethe University.

-
- [1] M. Gyulassy and X.-N. Wang, Nucl. Phys. **B420**, 583 (1994), nucl-th/9306003.
 - [2] C. Adler et al. (STAR), Phys. Rev. Lett. **89**, 202301 (2002), nucl-ex/0206011.
 - [3] K. Adcox et al. (PHENIX), Phys. Rev. Lett. **88**, 022301 (2002), nucl-ex/0109003.
 - [4] P. Huovinen, P. F. Kolb, U. W. Heinz, P. V. Ruuskanen, and S. A. Voloshin, Phys. Lett. **B503**, 58 (2001), hep-ph/0101136.
 - [5] L. P. Csernai, J. I. Kapusta, and L. D. McLerran, Phys. Rev. Lett. **97**, 152303 (2006), nucl-th/0604032.
 - [6] R. A. Lacey et al., Phys. Rev. Lett. **98**, 092301 (2007), nucl-ex/0609025.
 - [7] D. Molnar and M. Gyulassy, Nucl. Phys. **A697**, 495 (2002), nucl-th/0104073.
 - [8] D. Molnar and P. Huovinen, Phys. Rev. Lett. **94**, 012302 (2005), nucl-th/0404065.
 - [9] R. Baier, Y. L. Dokshitzer, A. H. Mueller, S. Peigne, and D. Schiff, Nucl. Phys. **B484**, 265 (1997), hep-ph/9608322.
 - [10] R. Baier, Y. L. Dokshitzer, A. H. Mueller, and D. Schiff, Phys. Rev. **C58**, 1706 (1998), hep-ph/9803473.
 - [11] M. Gyulassy, P. Levai, and I. Vitev, Nucl. Phys. **B594**, 371 (2001), nucl-th/0006010.
 - [12] S. Jeon and G. D. Moore, Phys. Rev. **C71**, 034901 (2005), hep-ph/0309332.
 - [13] C. A. Salgado and U. A. Wiedemann, Phys. Rev. **D68**, 014008 (2003), hep-ph/0302184.
 - [14] S. Wicks, W. Horowitz, M. Djordjevic, and M. Gyulassy, Nucl. Phys. **A784**, 426 (2007), nucl-th/0512076.
 - [15] Z. Xu and C. Greiner, Phys. Rev. **C76**, 024911 (2007), hep-ph/0703233.
 - [16] Z. Xu and C. Greiner, Phys. Rev. **C71**, 064901 (2005), hep-ph/0406278.
 - [17] Z. Xu, C. Greiner, and H. Stoeckler (2007), 0711.0961.
 - [18] Z. Xu and C. Greiner, Phys. Rev. Lett. **100**, 172301 (2008), 0710.5719.
 - [19] A. B. Migdal, Phys. Rev. **103**, 1811 (1956).
 - [20] M. Gluck, E. Reya, and A. Vogt, Z. Phys. **C67**, 433 (1995).
 - [21] A. Adare et al. (PHENIX) (2008), 0801.4020.
 - [22] J. Adams et al. (STAR), Phys. Rev. Lett. **91**, 172302 (2003), nucl-ex/0305015.
 - [23] O. Fochler, Z. Xu, and C. Greiner, forthcoming (2008).
 - [24] J. Adams et al. (STAR), Phys. Rev. **C72**, 014904 (2005), nucl-ex/0409033.
 - [25] G. L. Ma et al., Phys. Lett. **B647**, 122 (2007), nucl-th/0608050.
 - [26] B. Zhang, L.-W. Chen, and C.-M. Ko, Phys. Rev. **C72**, 024906 (2005), nucl-th/0502056.